October 2021

Hsp70 Phosphorylation: A Case Study of Serine Residues 385 and 400

Sashrika Saini
University of Massachusetts Amherst

HSP70 PHOSPHORYLATION: A CASE STUDY OF SERINE RESIDUES 385 AND 400

A Thesis Presented

By

SASHRIKA SAINI

Submitted to the Graduate School of the University of
Massachusetts Amherst in partial fulfillment of the requirements
for the degree of

MASTER OF SCIENCE

September 2021

Molecular and Cellular Biology

HSP70 PHOSPHORYLATION: A CASE STUDY OF SERINE RESIDUES 385 AND 400

A Thesis Presented

by

SASHRIKA SAINI

Approved as to style and content by:

_____
Lila Gierasch, Chair

_____
Andrew Truman, Member

_____
Peter Chien, Member

_____
Tom Maresca, Department Head
Molecular and Cellular Biology

ACKNOWLEDGMENTS

The path in science I have chosen is one that has been paved by many before me, whose shoulders I stand on. To them, I am eternally grateful for igniting a ravenous curiosity within me and allowing me to become a humble pupil of this discipline. This curiosity has become so integral to my being, it's hard to tell what the alternative would be.

Before anyone else, it's my parents, Lokesh and Jasbeer Saini, without whom I would have very quickly admitted defeat. Their tireless, unconditional support and have seen me through all my triumphs and challenges. It was at home where this inquisitive nature first took shape, and I was always encouraged to ask why.

In addition to the family I inherited, next I would like to express my gratitude to the family I acquired at UMass. At the heart of this family is Lila Gierasch, a mentor unparallel in her thinking, her tenacity, and frankly is a force to be reckoned with. Her steadfast guidance has shaped the way I think to an immeasurable degree, and for that I will be forever grateful. I am thankful to Eugenia Clérico and Wenli Meng for their patience and constantly challenging me to think critically. Being a part of the Gierasch lab has not only given me the privelege to work amongst incredible people, but also provided me with life-long friendships.

Next, I would like to professors Scott Garman, Ludmilla Tyler, and Amy Springer who have been instrumental in my success as an undergraduate and have continued to support me through my graduate studies. I thank my committee members, Andrew Truman and Peter Chien, for being critical and enthusiastic regarding my work. Their insights on this project have been invaluable and made the journey that much more exciting.

Lastly, I would like to thank Jianhan Chen and Erik Nordquist, without whom the MD simulation data presented in this work would be non-existent.

As I look towards this upcoming chapter in my life, I will take the lessons I have learned here and carry them with me in my practice, as I aim to develop into a thoughtful, inquisitive and compassionate doctor.

ABSTRACT

HSP70 PHOSPHORYLATION: A CASE STUDY OF SERINE RESIDUES 385 AND 400

SEPTEMBER 2021

SASHRIKA SAINI, B.S., UNIVERSITY OF MASSACHUETTS AMHERST

M.S., UNIVERSITY OF MASSACHUSETTS AMHERST

Directed by Professor Lila Gierasch

Molecular chaperones play a key role in maintaining a healthy cellular proteome by performing protein quality control. Heat shock protein 70s (Hsp70s) are a diverse class of evolutionarily conserved chaperones that interact with short hydrophobic sequences presented in unfolded proteins, promoting productive folding, and preventing proteins from aggregation. Most of the extensive research on chaperone examines mechanism, substrate promiscuity, and engagement with many co-chaperones. Only recently were chaperones recognized to be frequent targets of post-translational modifications (PTMs). Despite the recent rise in PTMs identified, the impact of these modifications on chaperone function, whether singular or in concert with other modifications, remains elusive. To investigate the impact of PTMs on chaperone function, we chose to characterize two sites of phosphorylation on the linker of HspA1, the stress inducible human Hsp70. To mimic these phosphoserines, we used aspartate as a phosphomimetic substitution for all experiments. Interdomain allostery ties together chaperone structure and function. Therefore, the impact of phosphorylation on interdomain allostery is probed using biophysical and biochemical techniques. Altogether, data suggest that phosphorylation of the linker and SBD destabilizes the chaperone, while shifting the population towards the docked state. This result alludes to a previously described region of the protein that uncouples domain docking from conformational changes in the substrate-binding domain. The cross-

communication between these phosphorylation sites reveals a novel, synergistic effect on chaperone structure and function.

TABLE OF CONTENTS

LIST OF TABLES

Table **Page**

LIST OF FIGURES

Figure **Page**

CHAPTER 1

INTRODCTION

1.1 *Protein folding in the cell*

A necessity of all living systems is their ability to transform amino acids, one of the fundamental components of living matter, into three-dimensional, functional shapes. Since Levinthal's thought experiment in 1969, there have been serious amendments to our understanding of protein folding[1]. The endpoint of a successful folding pathway yields a compact structure that is coupled to its function and productive interactions with partners in a crowded cellular milieu[2,3]. In the cell, once proteins are synthesized from the ribosome, folding is initiated in some cases co-translationally before the nascent chain has even been released from the ribosome[4]. Molecular chaperones can assist the journey of an unfolded protein to its native structure by increasing the efficiency of the process[3]. By acting as holdases and unfoldases, they can guide the kinetically trapped intermediates towards native conformation (Figure 1).

1.2 Molecular Chaperone Heat Shock Protein 70

To maintain the functionality of the proteome, cells use molecular chaperones systems such as 70 kDa heat-shock proteins (Hsp70)[5]. Originally identified to be overexpressed in the cytoplasm, nucleus, endoplasmic reticulum, and other cellular compartments in response to stressful conditions such as heat, nutrient loss, or oxidative stress, Hsp70s are conserved among all three domains of life and perform cellular roles under non-stress conditions[6]. Hsp70s assist in a large variety of processes including the prevention of protein aggregation, promotion of protein folding to their native states, and stabilization of partially folded conformers for translocation across biological membranes[7]. Given the many cellular roles that Hsp70s perform, it is not surprising that complications in Hsp70 operation can provoke the onset of neurodegenerative diseases such as Alzheimer's disease (AD), Parkinson's disease (PD), Huntington's disease (HD),

and several cancers[8]. As a result, Hsp70 have become popular therapeutic targets. Understanding how cells employ chaperone systems to rescue proteins from kinetic traps and eventual misfolding is imperative to determining the etiologies of these diseases.

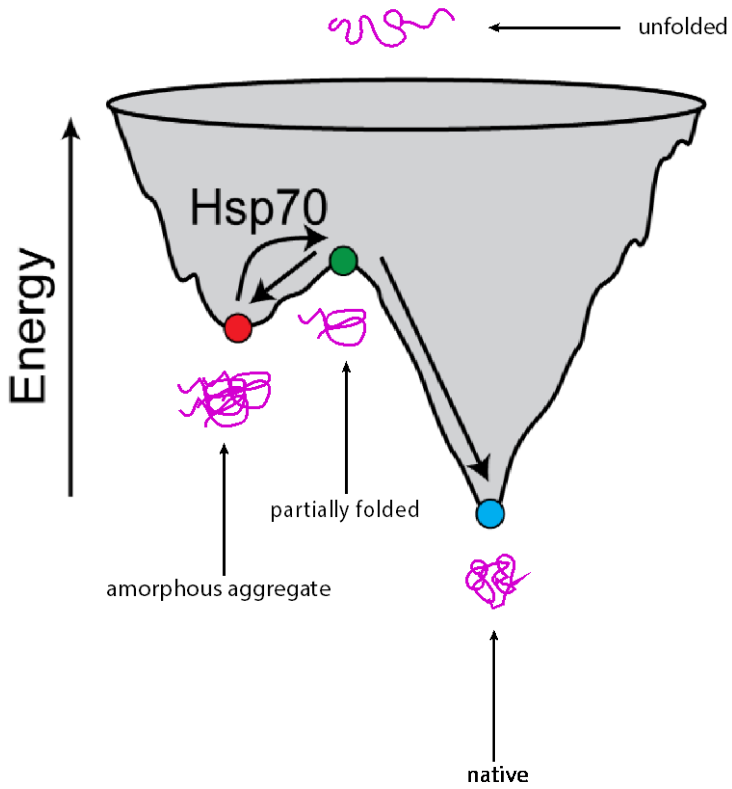

Figure 1.1 Unfolding model of molecular chaperone function. The protein folding funnel has energy on the y-axis, and conformation on the x-axis. A polypeptide enters the folding funnel in an unfolded state and can either spontaneously fold to the native state (blue dot; the global minima) or it can fall into a local minimum (red dot) in a misfolded or aggregate intermediate. Hsp70 can unfold the substrate and increase the probability that it will follow the energetically favorable path (Adapted from Smock, 2011)

The defining characteristic of Hsp70, pertinent to all its physiological roles, is its ability to bind a vast array of substrates. Although the mechanisms detailing all the functions Hsp70 performs are not completely clear, the substrate-chaperone binding has been extensively studied. Binding is achieved through the interaction of Hsp70s with short hydrophobic stretches of amino acids in the client proteins [9]. These hydrophobic motifs are usually buried in a protein's native state but become exposed to solvent when the protein is unfolded or misfolded (covered in greater detail below) [10]. Chaperone binding to these hydrophobe-rich sequences provides the substrate another opportunity to follow a more energetically favorable trajectory. Though there is no consensus sequence identified for Hsp70 substrates, algorithms developed on phage-display studies and peptide arrays can predict binding sites within the primary sequence of a protein[11,12]. Consistent with the many "housekeeping" functions Hsp70 has, a binding site appears at a frequency of one every 36 residues.

The peptides identified through the aforementioned studies elicited investigations of the molecular intricacies of Hsp70's canonical mode of binding. Past work has comprehensively characterized the structural details of binding at atomic-resolution, with model peptides substrates like NRLLLTG (NR)[13]. There are 5 distinct pockets in which residues in the peptide can fit into. The central (0^{th}) pocket is the most stringent, and consequently the most selective. Residues like Ile and Leu are highly favored in the 0^{th} pocket, whereas the remaining pockets are more accommodating[14]. The resulting phenomena is referred to as *selective promiscuity*. This feature is what enables Hsp70 to interact with a remarkably high number of clients in the cell and perform numerous functions.

1.3 Hsp70 structure and allosteric cycle

The functions of an Hsp70 are largely dictated by its structure and modulated by an intradomain allosteric mechanism. Hsp70s consist of two domains: a 45kDa actin-like nucleotide-binding domain (NBD) and a 25kDda substrate-binding domain (SBD) joined together by a highly conserved, flexible linker. The N-terminal NBD is made up of four subdomains (IA, IB, IIA, and IIB) that comprise lobes I and II. Adenosine nucleotides, ADP or ATP, bind in the groove between subdomains IB and IIB. All subdomains are involved in coordinating nucleotide and experience rearrangement upon binding and dissociation of nucleotide. These perturbations to the NBD subdomains allow the linker to nestle into lobe IIA upon ATP binding[15,16].

The SBD can be divided into two subdomains: the βSBD and the α-lid. The βSBD includes antiparallel beta sheets (β1-8) that are joined by loops ($L_{1,2}$, $L_{3,4}$, $L_{5,6}$, $L_{7,8}$) (Fig 1.2 C). The α-lid is formed by helices αA and αB, which have a characteristic bend between them in the undocked state but assemble into one continuous helix in the docked state[17]. Following helices αA and αB, the α-helical bundle is composed of helices αC, αD, and αE. Following the α-lid is a disordered C-terminal region (Fig 1.2 B). Strands β1 and β2, along with $L_{1,2}$, $L_{3,4}$ constitute the binding cleft. Substrate accessibility to the binding cleft is governed by ATP binding and hydrolysis.

Generally, in the presence of ATP, Hsp70s adopt a low substrate affinity state where the SBD is open and allows for rapid association and dissociation of a client peptide. The α-lid is docked onto the NBD, forming an additional NBD-SBD interface, and this conformation is referred to as the "domain docked" state. Upon substrate binding and ATP hydrolysis to ADP, where Hsp70 undergoes a massive conformational rearrangement where the two domains

disengage from one another, behaving in an independent manner ([14,18,19]). The SBD adopts a high affinity conformation in which the substrate-binding pocket closes, capturing the substrate. The

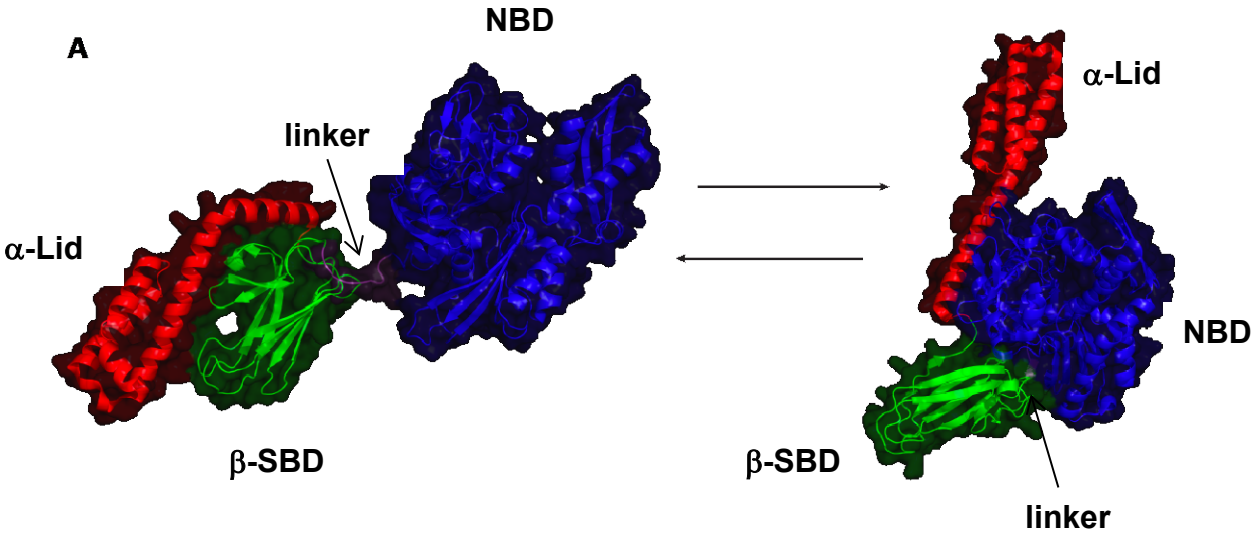

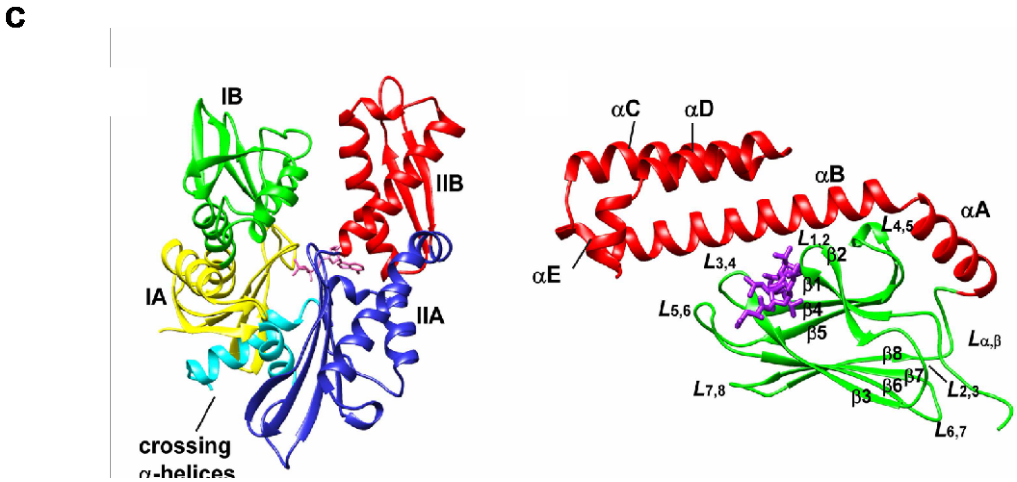

Figure 1.2. Hsp70 Architecture. (A) Crystal structures of DnaK in ADP bound state (PDB ID: 2KHO)[15] and ATP bound state (PDB ID: 4B9Q)[17]. **(B)** Schematic layout of the structural components of Hsp70 based on DnaK. **(C)** Subdomain breakdown of NBD (left) and SBD (right). ATP is bound in the NBD shown in pink. NRLLLTG peptide is bound to the SBD shown in purple. Panel C is taken from a review article[20].

a-lid closes on top of the βSBD, forming a α-lid-βSBD interface. This results in a low k_{off} rate and high affinity. The dynamic movement α-lid allows for the larger or unfolded substrates to bind in the canonical groove[21]. In this undocked state, NMR experiments and proteolytic lability of the linker indicate that it is quite solvent exposed and flexible[18,22]. Cycling between these two states remarks the allosteric behavior of Hsp70 and is the driving factor for all its functions. If we look beyond this two-state model, we can see that Hsp70 also samples an intermediate, allosterically active state, which propagates substrate binding and nucleotide exchange. This is a transient state that the chaperone visits when both ATP and substrate are bound. It was discovered by introducing a hydrolysis defective mutation (T199A) into DnaK [21,23]. In this state, the linker is still docked into the NBD, but the interface between the βSBD and α-lid is partially formed. ATPase activity and substrate off-rate are elevated (Fig 1.3).

Over time, abundant literature dissecting the allosteric communication between the SBD and the NBD has accumulated. In particular, the work done by Alexandra Zhuravleva and Eugenia Clérico in our lab encapsulates how allostery permits Hsp70 to see-saw between conformations[23]. An energetic balance is established between all the interfaces that are formed: α-lid-βSBD, α-lid-NBD, NBD-βSBD, and linker-βSBD or the linker-NBD. Ergo, an energetic tug-of-war between orthogonal interfaces, α-lid-NBD/ NBD-βSBD and α-lid-βSBD, dictate whether the chaperone will populate the undocked or the docked state[23].

While this energetic contest between interfaces decides the conformational fate of the chaperone, the structural components that facilitate communication between the two domains are the α-lid and the linker. In each given state, both can form contacts with one domain or the other. When in the undocked state, the α-lid tightly packs onto the βSBD through salt-bridges (as seen in DnaK) [13]. In the docked state, the α-lid conjoins with the NBD and forms a large interface[24].

The contact preferences of the α-lid influence the interactions that the linker, the other allosteric coupler, engages in.

The linker itself can be divided into semi-structured regions segmented with hinges that limit its distance and interaction with either domain. MD simulations from our lab suggest that there might also exist a transient interaction between the C-terminal part of the linker and the beginning of the SBD, which only occurs when the SBD is in the undocked state [25]. When the linker buries into the IIA lobe of the NBD upon ATP binding, it forms an antiparallel β-strand, perpetuating the signal through the SBD favoring vital residues to from contacts with the NBD[2126]. This further disrupts the β-sheet arrangement in the SBD, pulling apart strands β8 and β7, and disengaging the hydrophobic arch from the binding groove[27]. The linker binding to the NBD is also enough to stimulate ATP hydrolysis, for the eventual return to the undocked state[18,28]. Therefore, the linker is veritably a dynamic switch that couples together nucleotide and substrate binding for the Hsp70.

Though most of the work regarding Hsp70 has been done on the *E. coli* homolog, DnaK, many of defining features hold true for the eukaryotic counterparts. Despite a conserved mechanism, methyl-TROSY NMR analysis supplement with proteolytic susceptibility of the linker indicate that the allosteric landscape is very tunable. Wenli Meng, a senior research fellow in our lab, spearheaded a study comparing the landscape of DnaK with two cytoplasmic human Hsp70s, HspA1 and Hsc70, which have 46% sequence identity with DnaK and 86% sequence identity between each other. We learned that both human Hsp70s favor the domain-docked state for a significant portion of the allosteric cycle, whereas DnaK only visits the docked state when ATP is bound (Fig 1.3). Consequently, HspA1 and Hsc70 have much lower affinity for substrate and eventual binding of substrate minimally, if at all, stimulates ATP hydrolysis[29]. Intrinsic

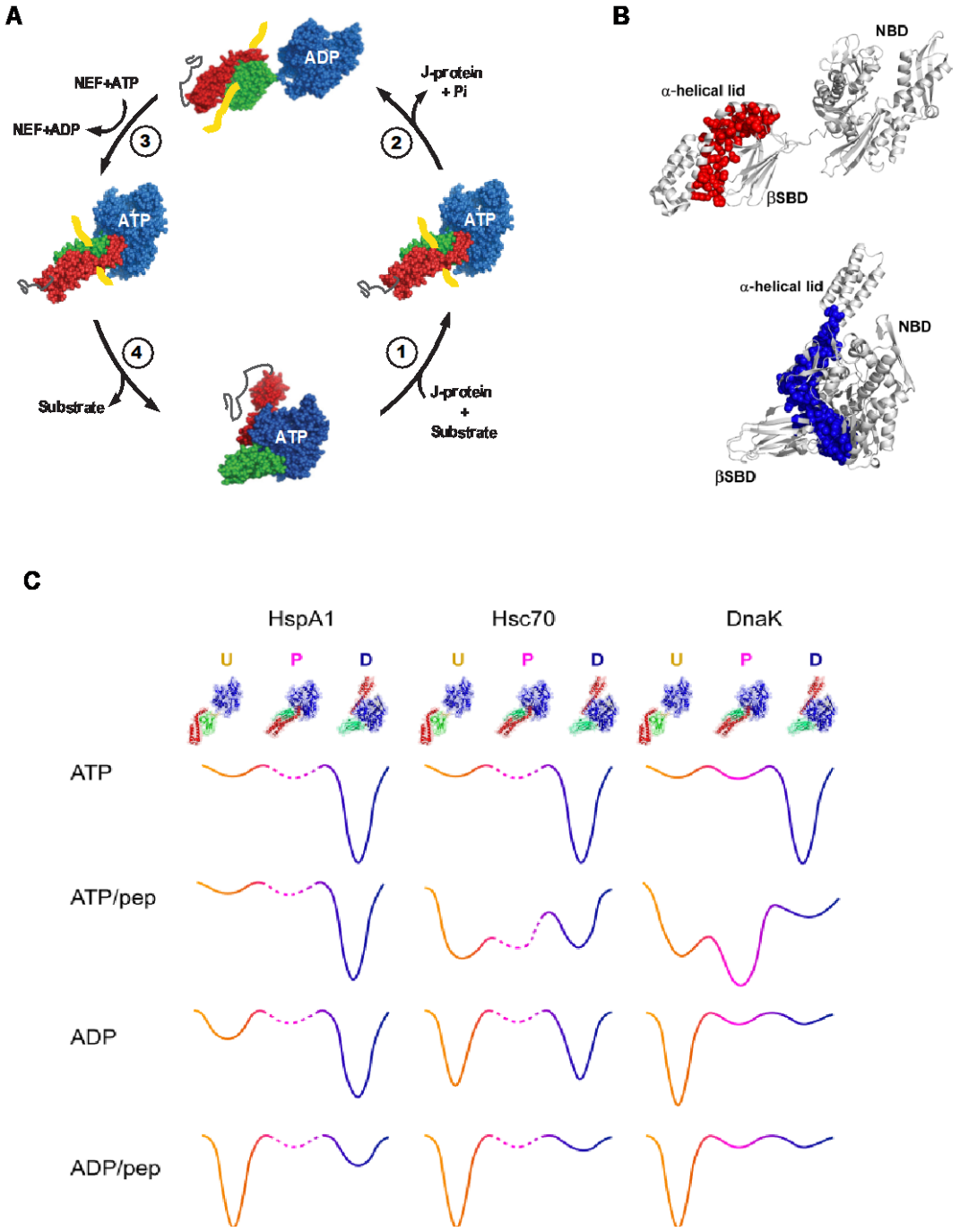

Figure 1.3. Allosteric regulation of Hsp70. (A) The allosteric cycle of Hsp70. Coloring mirrors the schematic in Figure 1B. **(B)** The orthogonal interfaces of Hsp70, βSBD-α-lid interface (red) in the undocked state, and NBD-SBD interface (blue) formed in the docked state participate in an energetic contest that governs the allostery of Hsp70. Panel B is reproduced from a review article[20]. **(C)** Allosteric landscapes of HspA1, Hsc70 and DnaK. U is undocked, P is allosterically active, and D is docked. Panel C is taken from a published article[29].

factors such as residue changes have evolutionarily modulated the allosteric landscapes of Hsp70, but there are also extrinsic factors such as co-chaperones that assist in wide spectrum of functions Hsp70 performs.

1.4 Co-chaperones assist in Hsp70 function

Hsp70s engage in many partnerships in the chaperone network that help facilitate the physiological functions they serve. Two of the major players are J-domain proteins (JDPs) and nucleotide exchange factors (NEFs). JDPs help sequester substrate, thereby stimulating ATPase activity, while NEFs promote exchange of ADP for ATP, thereby stimulating substrate release. JDPs are multifunctional family of proteins, named for the characteristic J- domain they all contain. A conserved motif, HPD (His-Pro-Asp), is required for stimulating ATPase activity in Hsp70, and contacts Hsp70 at the linker[30]. It has been proposed that J-domain binding to Hsp70 triggers undocking and transmits the allosteric signal through the linker to the NBD. This positions the NBD lobes optimally for hydrolysis of ATP[25,30].

Eukaryotic J proteins have more multifunctionality and are usually divided into the three classes (A, B and C). They are categorized based on the presence of a zinc-finger between the first two domains. In class A and B, the J-domain is at the N-terminus, but in class C, it can be anywhere. They can display both broad substrate specificity, while some are very narrow and perform specialized functions. JDPs are more numerous than Hsp70s, and it is possible that one Hsp70 might interact with many JDPs. As a result, the underlying cause of many of the protein misfolding diseases is due to a defect in JDPs [31].

The NEFs that interact with Hsp70 are much more diverse. The singular prokaryotic NEF, GrpE, works as a dimer to facilitate the dissociation of ADP by binding to subdomain II and releasing nucleotide[32]. This mechanism is conserved across eukaryotic NEFs, but they are

much more functionally diverse. Hsp110s are the most abundant and are structurally homologous to Hsp70s. Hsp110s require ATP binding to perform their function, but another class of NEFs, known as BAGs (BCL-2 associated anthanogene), do not. They are a class of structurally diverse NEFs which allows them to be involved in many specific cellular functions. They contain a ubiquitin-like domain which is useful in directing proteins to the proteosome for degradation. Perhaps the substrate in question dictates which BAG interacts with Hsp70[33].

1.5 The chaperone code

Aside from the collection of co-chaperones that accelerate the Hsp70 allosteric cycle and bring confer functional diversity to the chaperone, acquired features like post-translational modifications (PTMs) can also impart a regulatory function onto Hsp70s. In recent years, considerable efforts have gone into uncovering many PTM sites on Hsp70 using bioinformatics, proteomic approaches, and high-resolution MS. These include AMPylation, acetylation, ADP-ribosylation, methylation, ubiquitination, SUMOylation, and phosphorylation [34]. Phospho-proteomic studies, and a general "-omics" method has revolutionized the discovery of PTMs, and has exposed a *chaperone code*, the complex collective of all identified on Hsp70.

With regards to phosphorylation, nearly 88 phosphorylation sites have been identified on Hsc70, along with similar numbers on the ER and yeast Hsp70s. Although a significant number of "proteinopaties" stem from inappropriate phosphorylation events, the number of P-sites with associated functions is not commensurate with the number discovered. A few case studies have emerged, detailing the roles of Hsp70 phosphorylation in the cell cycle, cancer progression, and client triage[34].

1.6 Phosphorylation of Hsp70's prominent allosteric coupler

One of the studies that explored phosphorylation looked at the two sites one on the linker, Serine 385 (S385) and one that lies adjacently in the SBD, Serine 400[35]. This study explores these in HspA1, but phosphorylation of these residues is conserved in many homologs and human isoforms of Hsp70 (Fig 4). Cells that were treated with epidermal growth factor were shown to trigger phosphorylation of HspA1, through extracellular signal-regulated kinase (ERK). Although this kinase is likely to be involved in the pathway, other studies contest that these sites do not match the typical ERK substrate requirements (ref). The authors identified these phosphorylation sites by performing an in-SDS-PAGE digest and subjecting that sample to LC-MS. The spectra do indicate that both S385 and S400 are phosphorylated but the MS data does not support the fact that they are simultaneously phosphorylated. Despite this, rest of the study investigates the cellular and functional impact of a double S385D/S400D phosphomimetic HspA1. The mutation to aspartate is representative of phosphorylation as it is a residue with larger, negative character. The functional studies examining luciferase folding activity and substrate affinity are done in apo state, which negates the allosteric impact of nucleotide. The authors observe that the S385D/S400D mimic has only ~1.5 times higher substrate affinity and folding activity. This minimally compelling observation was corroborated by a limited proteolysis experiment that was performed in presence of ATP. The proteolysis experiment confirmed that the two domains favor the undocked conformation, which presumably would result in a higher folding activity and substrate affinity. This result is puzzling as in the ATP state, HspA1 highly favors the docked state. Despite the highly conserved mechanism of Hsp70s, the allosteric landscape and stimulation of ATPase activity by substrate binding differ between homologs (ref). The inconsistent use of nucleotide in these experiments, and an overgeneralization of Hsp70 allostery leaves room for limited analysis.

In cell ectopic expression of phosphomimetic and mutant HspA1 (S385A/S400A) showed increased and decreased cell viability respectively, in relation to WT HspA1. Moreover, S385D/S400D shows little to no response in presence of inhibitor VER155008 (VER) that targets the ATP binding cleft, whereas the activity of both WT and mutant HspA1 were both

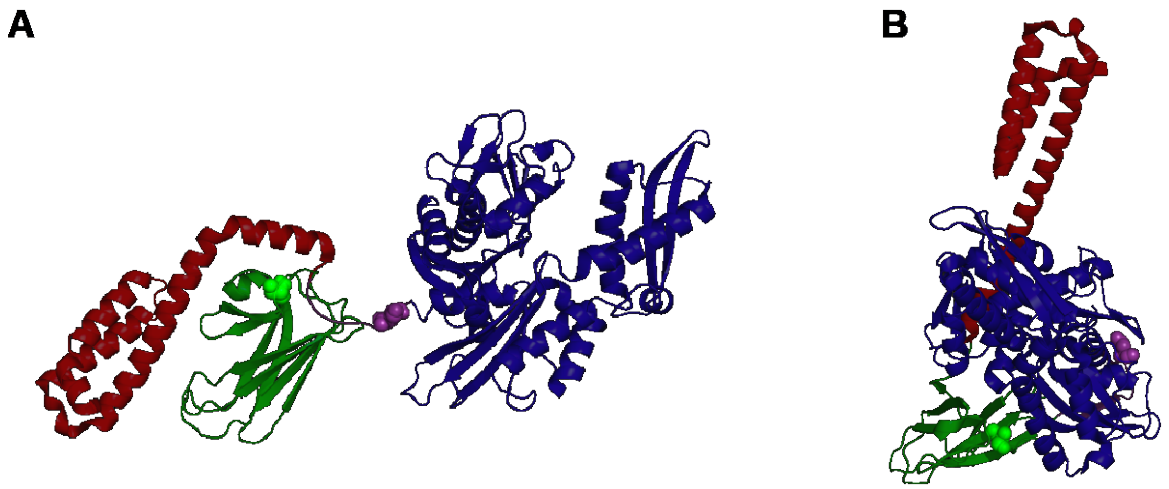

C

	381	385	400	405
DnaK	TGD----VKDVLLLDVTPLSLGIETMG			
HspA1	MGDKSENVQDLLLLDVAPLSLGLETAG			
Hsc70	SGDKSENVQDLLLLDVTPLSLGIETAG			
SSA1	TGDESSKTQDLLLLDVAPLSLGIETAG			
SSA2	TGDESSKTQDLLLLDVAPLSLGIETAG			
SSA3	TGDQSTKTQDLLLLDVAPLSLGIETAG			
SSA4	TGDQSSTTQDLLLLDVAPLSLGIETAG			

Figure 1.4. EGF dependent phosphorylation of HspA1 on interdomain linker and substrate binding domain. **(A)** Structure of ADP bound DnaK (PDB ID: 2KHO). Phosphorylation sites 385 and 400 are highlighted in spheres. **(B)** Phosphorylation sites shown on ATP bound DnaK. Coloring follows schematic in Figure 1B. **(C)** Multiple sequence alignment between Hsp70 homologs. Known phosphorylation sites on the linker of eukaryotic Hsp70s and DnaK are highlighted in yellow (GPM database).

decreased. Ultimately, the authors conclude that this phosphomimetic version of HspA1 might represent a pathological form present in cancer cells, as the presence of melanoma cell-line expressing the phosphomimetic had augmented cell proliferation. It is evident that phosphorylation on a structurally and allosterically invaluable segment of HspA1 has tantalizing in-cell consequences.

1.7 Statement of Thesis

The stunning array of functional diversity that marks the essence of chaperone Hsp70s is mediated by an energetically driven allosteric landscape. This promiscuous protein machine maintains a delicate balance between many conformational states as it imparts stability to a variety of clients. We have learned of many reciprocal relationships that give way to this phenomenon: substrate-binding and domain-docking, nucleotide binding and substrate affinity. Several intrinsic factors, for example, evolutionary residue changes among Hsp70 homologs, facilitate tuning of this allosteric cycle.

Until now, the prevailing view was that Hsp70 abundance in the cell was regulated by stress response. Past work has extensively focused on understanding the chaperone through its co-chaperone network, ATP-driven allosteric mechanism, and its extensive clientele. Recent advances in proteomics have revealed the diversity with which Hsp70s are heavily modified post-translationally. This array of post-translational modifications has the potential to modulate extrinsic factors like co-chaperone interactions, localization, substrate selectivity. Moreover, PTMs can also impact intrinsic properties of the chaperone. The inherent allostery in Hsp70s serves as an excellent candidate for assessing the effect of post-translational modifications, as it orchestrates the critical cellular functions the chaperone performs. The increasingly large number of PTMs being discovered begs the question: What role do these PTMs play in regulation of the

chaperone? How do PTMs perturb the allosteric landscape of Hsp70s? Specifically, how does the phosphorylation of two specific Serine residues, S385 and S400, lend tunability to the chaperone? To extend the work done by Lim et al. on these sites, it becomes critical to separate these two serine residues and assess their contribution to the S385D/S400D phosphomimetic of HspA1. If we adopt a broader vantage point, it becomes imperative to ask: What is the PTM-induced cellular chaperone response?

Chapter 2 of this thesis delineates the functional and structural differences between wildtype HspA1 and the linker phosphomimetic mutants: S385D, S400D, and S385D/S400D. An investigation of these mutants through circular dichroism indicates that phosphorylation destabilizes HspA1. In accordance with that, substrate binding affinity is reduced, despite indications from proteolysis that phosphorylation favors the undocked conformation.

CHAPTER 2

PHOSPHORYLATION OF THE LINKER AND SUBSTRATE BINDING DOMAIN DESTABILIZES HSPA1.

2.1 Introduction

Preliminary work done on phosphorylation sites S385D and S400D leaves us with tempting results yet leaves several questions about the structural and functional impact of phosphorylation unanswered. Considerable work has previously been done to dissect the allostery of Hsp70s, using DnaK as a model. Anastasia Zhuravleva, a former member of the Gierasch lab extensively explored the role of specific regions in the SBD in interdomain allostery. Her work investigates how the βSBD mediates two-way negative allostery: substrate binding disfavoring upon domain docking, and domain docking disfavoring upon substrate binding. Using the DynDom algorithm, it was established that the βSBD undergoes a subtle rearrangement upon ATP binding that perturbs key interface residues. The two dynamic domains involved in this structural transition are subdomain I (resides 420-437 and 456-485) and subdomain II (residues 400-419 and 440-455). Subdomain II is of particular importance, as it has two highly conserved residues, Lys414 and Asn415, that make contacts with the NBD: T221 and D326. Movement in the SBD creates distance between K414 and N415. Chemical shift perturbation (CSP) analysis and MD simulations indicate that these interface residues experience a lot of flexibility and sensitivity to even soft mutations. Given that K414I, an allosterically defective mutation, enables DnaK to populate the allosterically active state, interactions that agitate this allosteric hot spot will likely shift the conformational landscape of Hsp70.

2.2 Results

2.2.1 Residues S385 and S400 make contacts with allosteric hotspots

To elucidate the functional and structural basis of regulation that is exerted on HspA1 via phosphorylation, we created a homology model of HspA1 in the domain docked state using DnaK (PDB 4B9Q) as a template. Eukaryotic Hsp70s share 49.83% sequence identity with their *E. coli* homolog, but sectors deduced to be participating in inter-domain allosteric communication are highly preserved. The SWISS-MODEL algorithm was used to create a homology model that covers residues 4-610 with a global model quality estimate (GMQE) of 0.74. The homology model of ATP-bound HspA1 (Fig 2.1A) and the crystal structure of the substrate binding domain of HspA1 (PDB 4PO2) was used to probe the neighborhood of phosphorylation sites S385 and S400. The HspA1 SBD structure starts at residue 386, which is part of the tail end of the linker exposed when the chaperone is in the undocked conformation. Superimposition of homology model with PDB 4B9Q yields an RMSD value of 1.885 when residues 380-555 are fixed. This selection includes the entire linker and the end of the HspA1 target sequence used to produce the homology model.

In the undocked state, the R-group -OH of S400 forms a bifurcated hydrogen bond with the backbone -NH_2 of R416 and the side chain -O in the carbonyl of E446. The carbonyl group of E446 makes a hydrogen bond with the amine of S400, whereas G445 makes a hydrogen bond the backbone carbonyl of S400.

In a docked conformation, S400 is observed to be directly contacting only G445 and E446. Residue S385D falls in the flexible region of the linker and participates in limited interactions, namely an electrostatic bond with the backbone amine of the neighboring glutamate.

In both states, docked and undocked, S400 is found contacting important allosterically active residues which can be expected to have local and global effects upon phosphorylation.

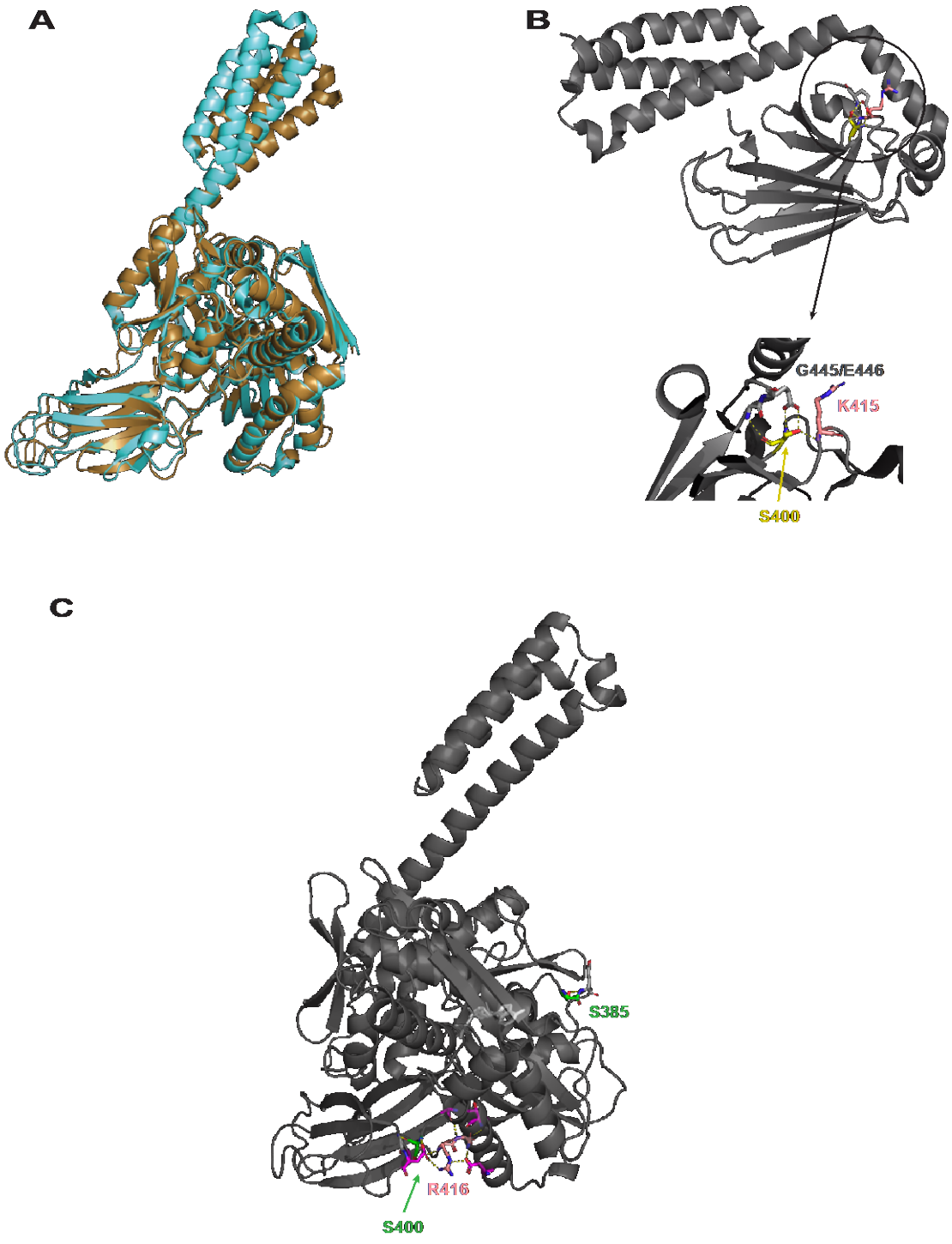
A
B
G445/E446
K415
S400
C
S385
R416
S400

Figure 2.1. Phosphorylation site S400 involved in hydrogen bonding network with allosterically critical residues. (A) Homology model of ATP-bound HspA1 based on DnaK. Model (gold) is superimposed on DnaK (PDB ID: 4B9Q). **(B)** Crystal structure of HspA1 SBD highlighting S400D and H-bonds with neighboring residues in subdomain II. **(C)** Hydrogen bonding network of S400 and S385 in the homology model of ATP-bound HspA1. Residues making polar contacts with R416 shown in pink.

2.2.2 Phosphorylation of the interdomain linker and SBD of HspA1 increase in vivo degradation

As previously suggested, Hsp70 adopts an undocked conformation upon phosphorylation at two specific sites: S400 and S385[35]. These fall in the SBD and the linker, respectively. In accordance with that result, purification of both wildtype Hsp70 and the corresponding phosphomimetic mutants revealed that the mutants were much more susceptible to proteolysis in cell and in solution than wildtype. Supplementation with a protease inhibitor cocktail (see Methods for details) was recommended to prevent cleavage *in situ* and during subsequent chromatography steps to ensure minimize the effects of any residual proteases that escaped separation from the protein of interest[36]. Wildtype HspA1 remains stable throughout the purification with negligible proteolysis as seen in the elution fractions (Fig 2.1A). On the other hand, mutants display cleavage into successively shorter truncations of the original 61.5 kDa construct. Taken together, the low overall yield of the phosphomimetic constructs can be explained by their instability in comparison to their wildtype counterpart.

2.2.3 Use of adenosine nucleotide enhances stabilization of HspA1 during purification

The conformational landscape of Hsp70 is modulated by an energetic game of tug-of-war as previously suggested by Zhuravleva et al., where the opposing players are the two inter-domain interfaces. In the case of HspA1, the domain-docked state is the clear winner, and is favored more than 80% of the time.[23,29]. Strikingly, HspA1 strongly prefers the NBD-SBD docked conformation even in the ADP-bound state[29]. Therefore, it is likely that adding an excess of ATP or ADP stabilizes Hsp70 by promoting

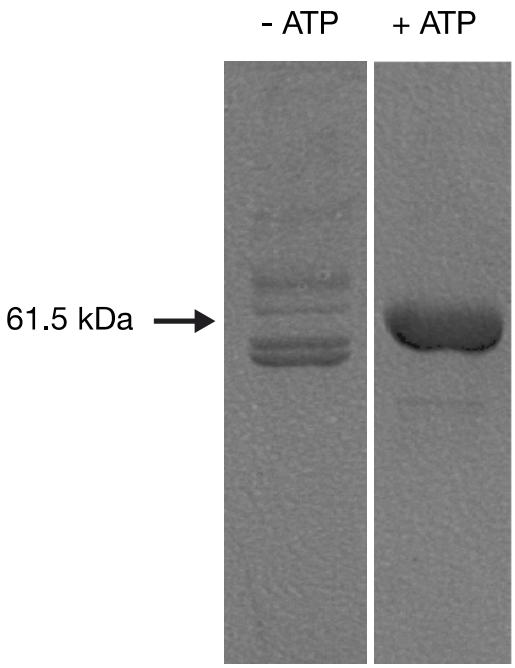

Figure 2.2. Mutant S385D/S400D stabilized by ATP during purification. In the purification without excess ATP, there is minimal amount full-length protein (61.5 kDa). In the presence of ATP, the elution fraction contains a significantly greater proportion of full-length S385D/S400D.

domain docking. The presence of a single, strong band at 61.5kDa for the elution fractions of mutants S385D/S400D and S400D qualitatively confirms that there was less proteolysis. This points to the possibility that the NBD may be more vulnerable to proteases in the apo state, and the addition of nucleotide exerts a stabilizing effect.

2.2.4 HspA1 becomes more proteolytically labile upon phosphorylation

To investigate the impact of phosphorylation on the conformational landscape of HspA1, we conducted a limited proteolysis assay, suspecting the linker region would more exposed and accessible to proteinase K, which was previously demonstrated by Lim et al[35]. All experiments were performed under ADP-bound conditions. As expected, wildtype Hsp70 was protected from proteinase K for the longest length of time and retains the greatest percentage of full-length (1-555) construct by the 15-minute time point (Fig 2.3A). At the zero-minute time point, Wildtype HspA1 sample is comprised of 94.7% of the 61.5kDa (full-length) construct and a cumulative 5.3% of various bands ~ 45kDa, which is approximately the size of the NBD (Appendix Fig 1A). At 15 minutes, 17% of the incubated sample is full-length, greatest amongst all HspA1 constructs. This resistance to proteinase K is consistent with previous findings that HspA1 favors a docked conformation in the ADP-bound state[29]. The two-domain construct of S385D persisted for 10 minutes before being degraded into its individual components, SBD and NDB; S400D was only resistant to proteinase K for 5 minutes. Both single mutant constructs had trace amounts of full-length bands at the 15-minute mark. In addition to WT, both single mutants show an increase in the NBD band relatively proportionate to the decreasing full-length band (Fig 2.3A, Appendix Fig 1A, 1B). The S385D/S400D mutant showed the most drastic difference between the 5-minute and 10-minute time point and rapidly declined as time progressed.

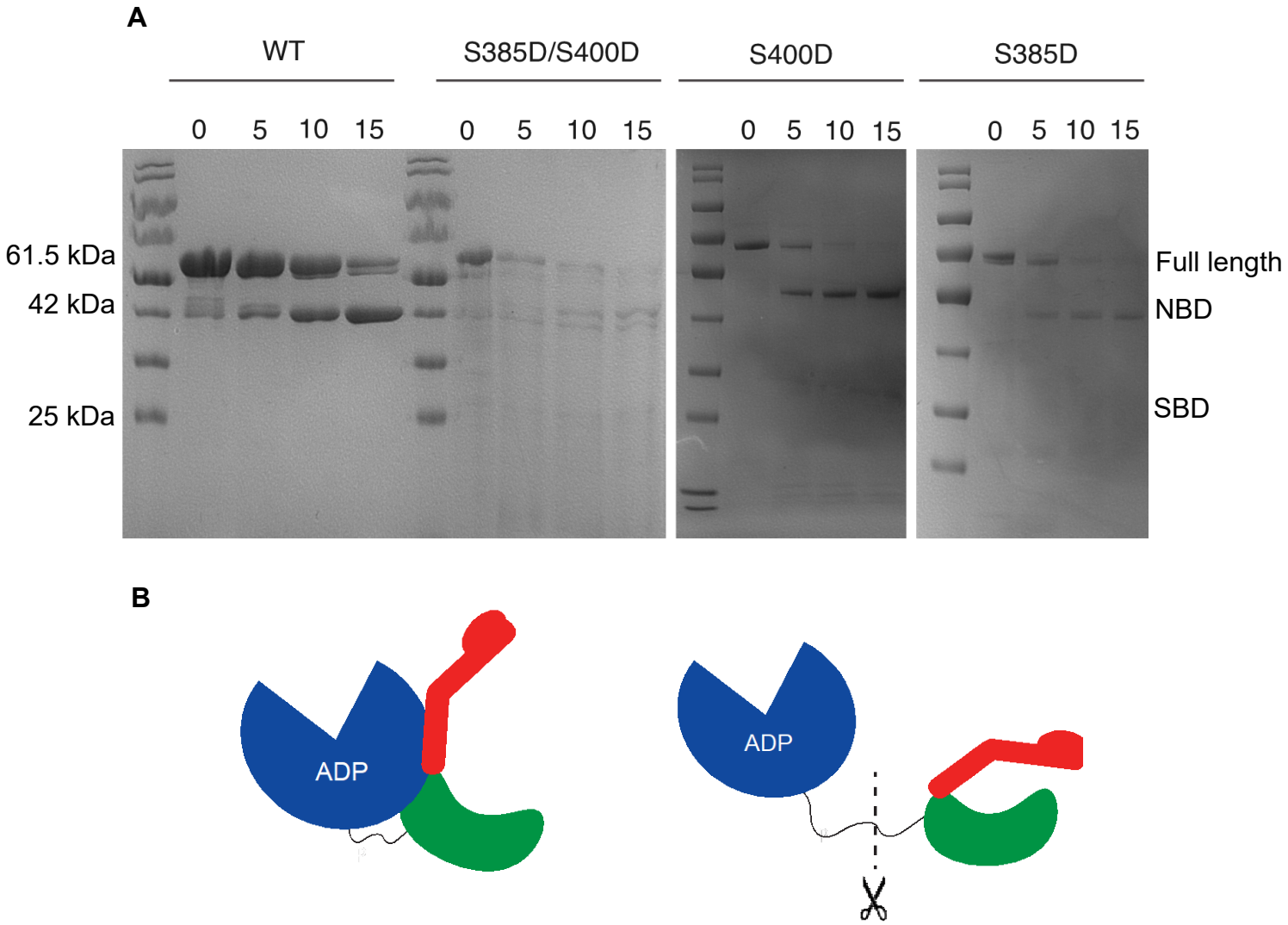

Figure 2.3. Phosphomimetic mutants of HspA1 show differences in susceptibility to proteolysis. **(A)** SDS-PAGE of limited proteolysis of WT, S385D/S400D, S385D and S400D at 15 min reaction time. **(B)** Schematic of cleavage by proteinase K: the left panel shows the docked form of the chaperone with lesser proteolytic vulnerability. The right panel shows the undocked form which is more susceptible to cleavage at the linker.

Additionally, the NBD shows dramatic degradation and instability. A disproportionately less amount of NBD is visible at the 15-minute time point in comparison to the amount of full-length construct at the start of the experiment (Fig 2.3A). From the loss of band intensity for the double phosphomimetic mutant, it can be argued that it is more unstable than WT or single mutant, as it is much more proteolytically labile. The distinctions between S385D and S400D are more subtle, and their rate of proteolysis falls somewhere between that of WT and S385D/S400D.

2.2.5 Phosphorylation decreases HspA1 affinity for substrate

Chaperone affinity for substate can be a functional assessment of interdomain allostery (ref). The molecular machine's use of nucleotide to cycle through its high-affinity and low-affinity states for substrate can be a measure of the reciprocal communication between the SBD and the NBD (ref). We believe the clathrin peptide serves as a suitable probe for measuring binding affinity, as it behaves anisotropically when bound to protein versus when it's free in solution (See Methods 2.4.2, 2.4.5). HspA1 is known to have significantly lower binding affinity to peptides in comparison to its eukaryotic counterpart Hsc70 and homolog DnaK[29]. The chaperone-peptide complex does not reach a saturation point, therefore, an exact K_D value cannot be extracted from the data. Nonetheless, WT HspA1 has the greatest affinity for clathrin, with an apparent K_D of 7.32 ± 0.91, approximately 5-fold greater S400D/QL and S385D/S400D/QL (Table 1). It can be concluded that a low affinity for substrate indicates a shift in the protein conformation towards the docked, low-affinity state.

2.2.6 Phosphomimetic substitutions synergistically destabilize chaperone

To interrogate the structural integrity of each of the mutants, circular dichroism was used to assess the secondary structure. The WT profile has minima at λ_{210} and λ_{220} of approximately -

8400 and -9000 (mdeg cm^2 $dmol^{-1}$). This is characteristic of alpha-helical content[37], and HspA1 is predicted to contain approximately 36% alpha-helical content (STRIDE)[38].

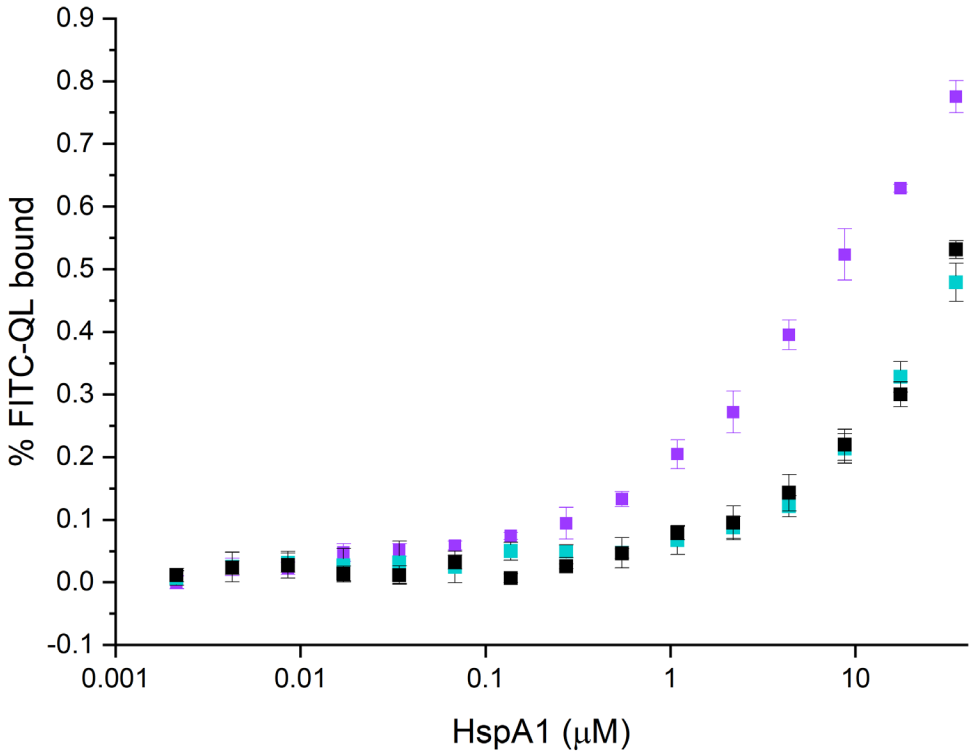

Figure 2.4. Phosphomimetic HspA1 constructs exhibit lower substrate binding affinity as compared to wildtype. Binding affinities of FITC labeled QL to WT HspA1 (purple), S400D (black) and S385D/S400D (cyan). K_D values are listed in Table 1. Error bars are from three technical replicates.

Table 1. Affinity values of HspA1 constructs

Construct	K_D
WT	7.32 ± 0.91
S400D	32.5 ± 0.45
S385D/S400D	35.0 ± 0.95

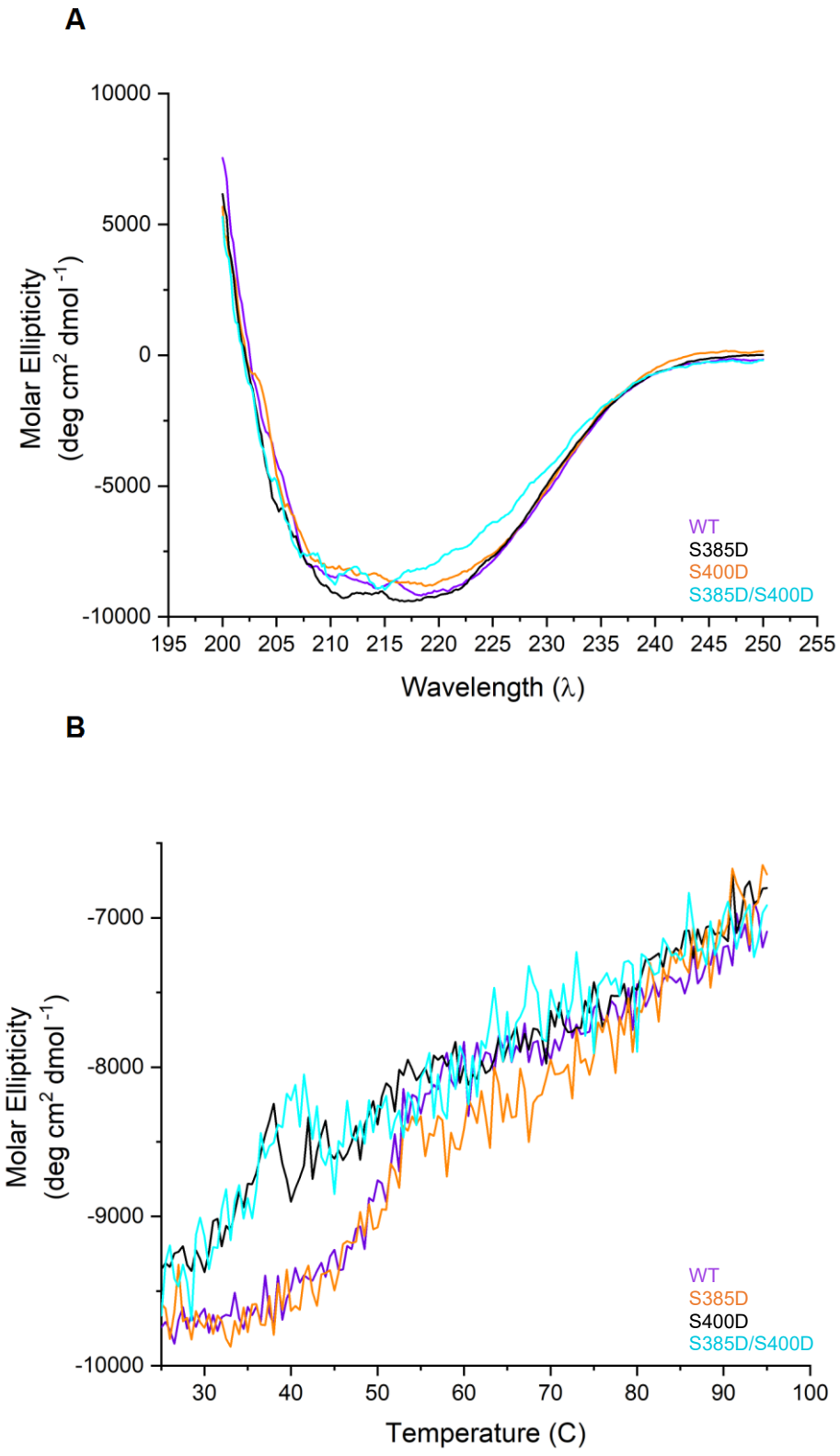

Figure 2.5. Destabilization of S400D and S385D/S400D revealed despite minimal changes in secondary structure. (A) Circular

Dicroism spectra of WT HspA1, phosphomimetic mutants, and DnaK 1-552YE from 200 nm to 250 nm. Thermal Scan of WT HspA1 and phosphomimetic mutants at 220 nm. All samples were measured with 100μM ADP.

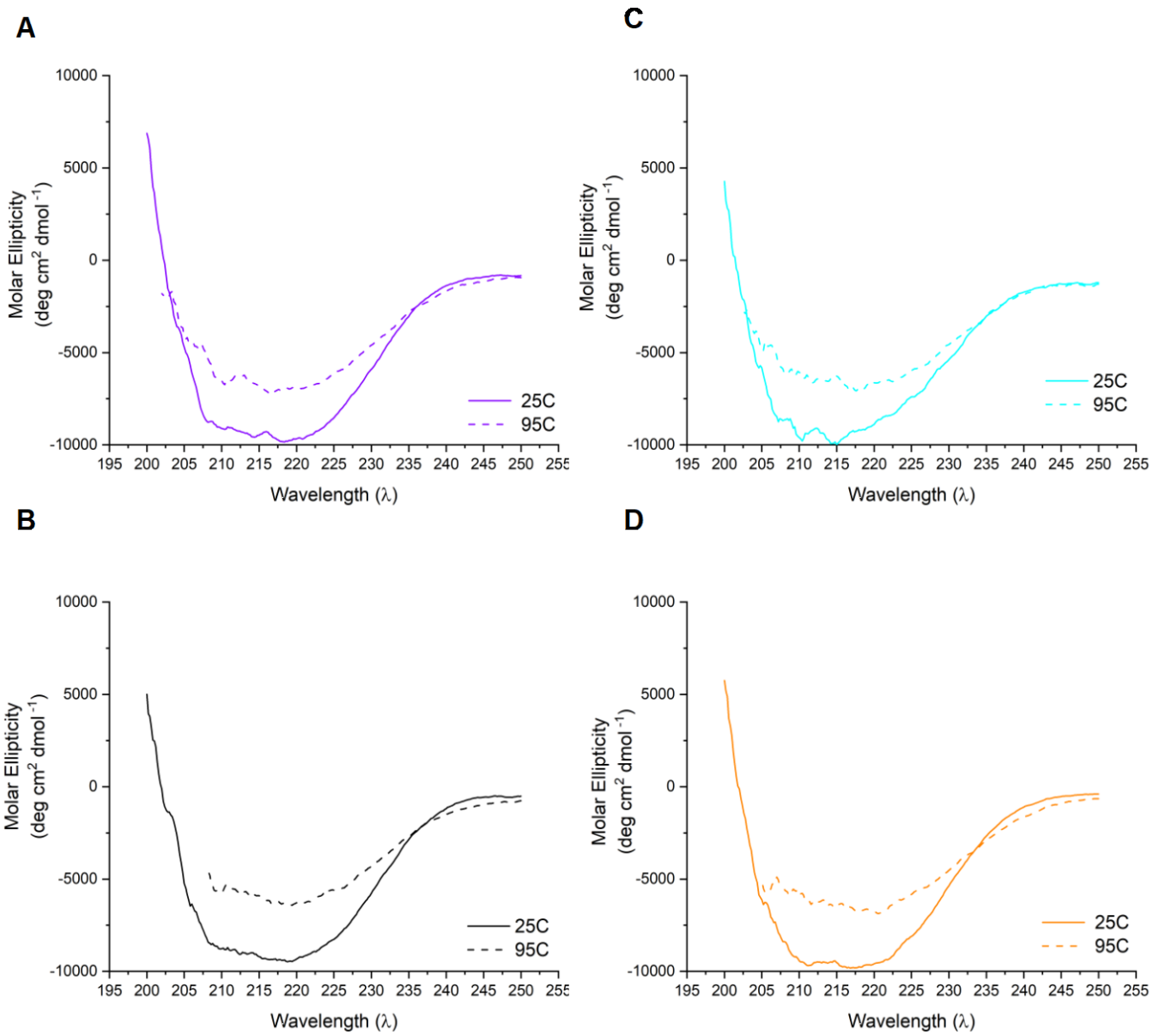

Figure 2.6. HspA1 mutants largely retain secondary strucure upon melting. (A) Circular Dicroism spectra of WT HspA1 200 nm to 250 nm. **(B)** Circular Dicroism spectra of S400D from 200 nm to 250 nm. **(C)** Circular Dicroism spectra of S385D/S400D from 200 nm to 250 nm. **(D)** Circular Dicroism spectra of S385D from 200 nm to 250 nm. All samples were measured with 100µM ADP. Spectra taken at 95˚C only include the data points ≤600 HT.

Single mutant S400D exhibits a similar shape to both WT and S385D, albeit shallower minima. The spectrum for S385D/S400D also displays secondary structure like WT HspA1, although the trace is poorly aligned with others in the well between λ_{208} and λ_{222} (Fig 2.5A). Overall, this result is indicating some wildtype structural features are preserved, but there might be some minor fluctuations in the native fold. This shift points to a change in secondary structure caused by the substitution of serine for aspartate and is likely the result of an alteration in the way residues are packed in the SBD. A thermal scan of WT and phosphomimetic mutants (Fig 2.5B) shows a small change in ellipticity as the temperature was increased from 25˚C to 95˚C. Despite the noise in the trace, two observations are evident. WT and S385D show a sigmoidal, cooperative denaturation, while S400D and S385D/S400D show a more continuous slope. The midpoint of the "inflection" for S400D and S385D/S400D is lower compared to WT and S385D. Despite gradual melting, all HspA1 constructs maintain some degree of the native fold (Fig 2.6 A-D). These findings lend themselves to the interpretation that S385D/S400D represents a synergistic effect of both individual substitutions on secondary structure, but S400D majorly contributes to the destabilization of S385D/S400D.

2.2.7 Phosphorylation shifts the population of HspA1 towards the docked state

A preliminary molecular dynamics simulation of ATP-bound of HspA1 was performed to dissect the local and global consequences of phosphorylation at two sites on HspA1. The trajectories of HspA1 WT and HspA1 phospho-Serine 400 were examined for 100 ns. A trace of root mean square deviations (RMSD) reveal dynamics of the entire protein molecule as a function of time. RMSD of the backbone atoms was calculated in a 15Å region surrounding residue S400. Wildtype HspA1 experiences a greater range of flexibility between 10 and 80 ns

that have an average magnitude of 1Å. Towards the end of this short simulation, both WT and phospho-Serine 400

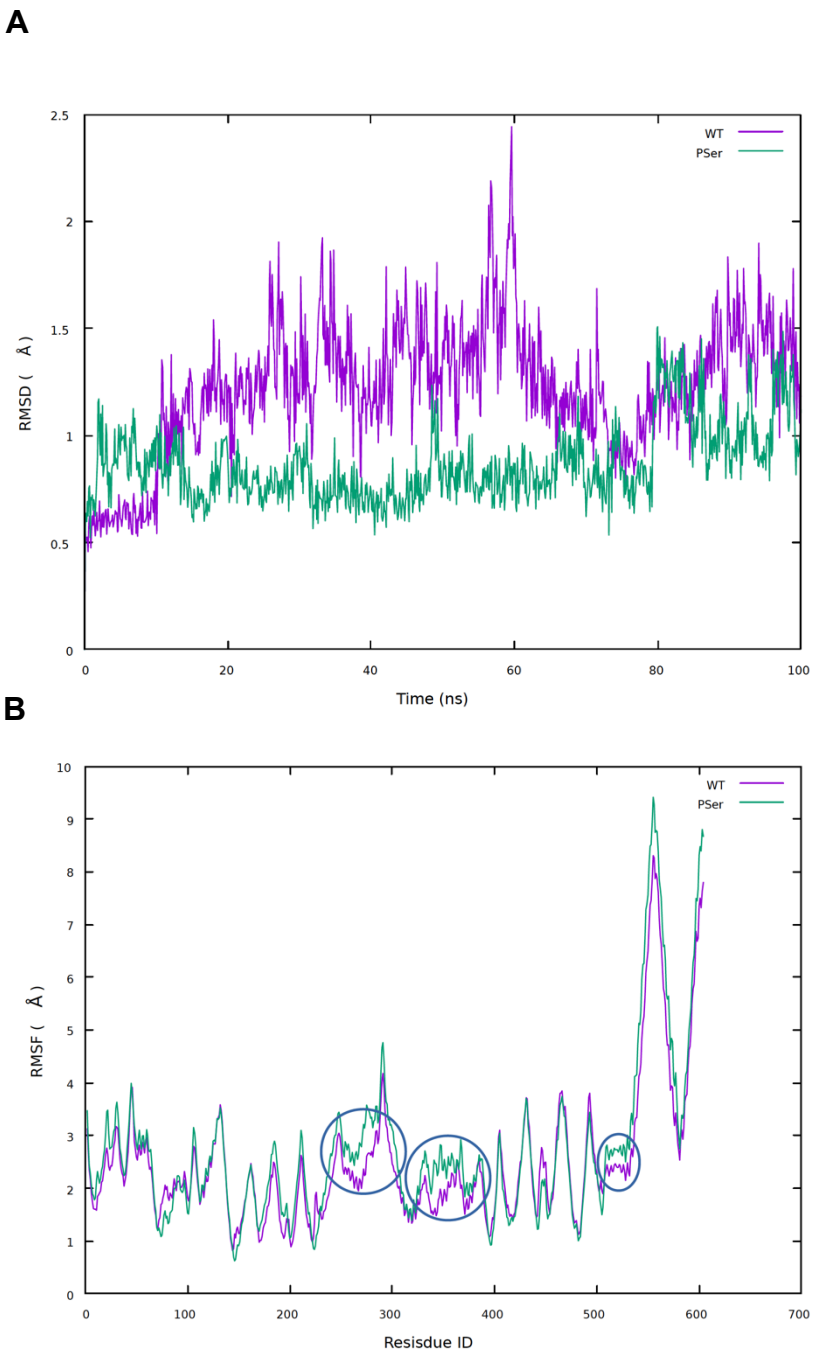

Figure 2.7. HspA1 dynamics upon phosphorylation of serine 400. (A) Root mean square deviations of backbone atoms in a 15 Å radius around S400. **(B)** Root mean square fluctuations over 100 ns by residue. Regions of great deviation between WT and PSer 400 are circled in blue.

trajectories equilibrate (Fig 2.7A). In contrast, the root mean square fluctuations (RMSF) show 3 distinct regions where phosphor-Serine 400 experienced greater fluctuations as a function of residue number: ~220-300, ~320-380, ~510-540 (Fig 2.7B). Superimposition of HspA1 WT and phospho-Serine 400 at 100 ns resulted in an RMSD value of 2.504 and shows deviations in both in the SBD and helices in subdomains IB and IIB (Fig 2.8A). Marginal deviation between the two protein objects in the green circled region indicate that the interface between the SBD and NBD in that region are packed more tightly in P-ser 400 (Fig 2.8A). Upon further examination, the region S400 in the βSBD and the proximal helix of the NBD that creates the βSBD-NBD interface are discernably closer together at the 100 ns timepoint for HspA1 phospho-Serine 400 protein. Closer inspection at key interface residues shows an expansive H-bonding network and rotation of residues S400, K415, R416, and E446 R-groups towards the NBD (Fig 2.8B). These differential trajectories unveil intriguing features of HspA1 dynamics as a consequence of phosphorylation.

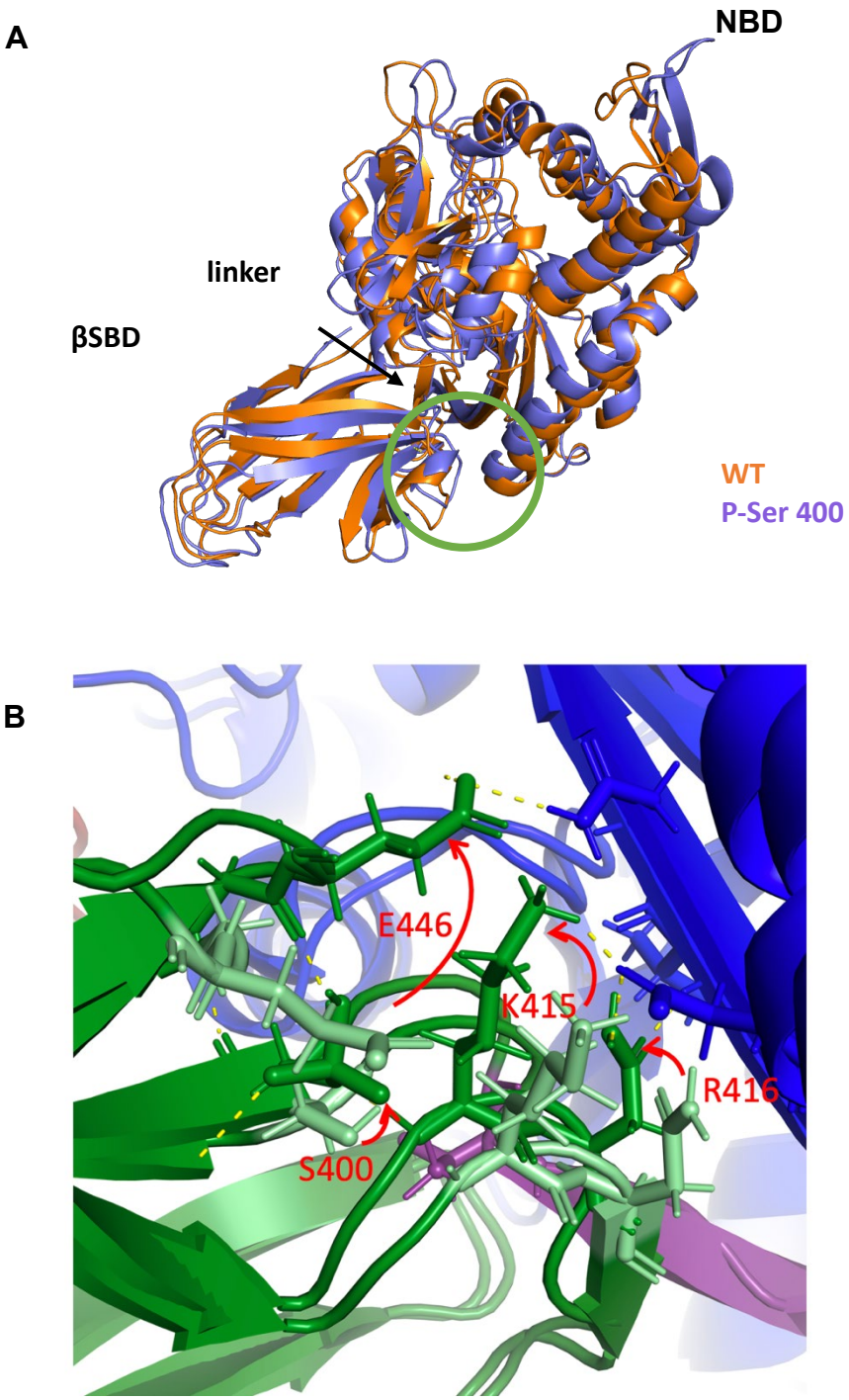

Figure 2.8. Structural changes resulting from the phosphorylation of serine 400. (A) Superimposition of WT HspA1 (Orange) and P-Ser 400 HspA1 (Purple). These structures are based on PDB: 5nro. **(B)** H-bonding network (yellow dashes) between NBD (blue) and SBD for residues 400, 415, 416, and 446. WT HspA1 (light green) is superimposed on P-Ser 400 (dark green) and the linker is shown in purple.

2.3 Discussion

Hsp70 function is allosterically driven and is defined by the resulting conformational landscape that is highly tunable. Evolutionarily conserved residues that reside in allosteric hotspots play key roles in tuning chaperone function. K414/R416 is a conserved site that experiences a rearrangement as β-SBD subdomain II rotates upon ATP binding. This shift couples conformational changes in the SBD with inter-domain docking as these residues pull away from intra-β-SBD contacts to form interaction on the NBD-β-SBD interface[27]. Interface residues R416 and N417 stabilize the docked state by being the link between NBD residues (T221 and D323) and more importantly, intradomain residues of the SBD (E446 and A397). Past work has shown that mutating these key residues has propagated perturbations widespread throughout the β-SBD in addition to local changes near the mutation site. Specifically, our lab identified that the soft K414R mutation causes ripple effects measured in CSP responses through to the αLid [27]. Prior work like this defines the underpinnings of what we refer to as the "tunability" of Hsp70s.

Covalent modifications like phosphorylation can be an external factor that modulate the architecture and by consequence, the dynamics of the chaperone. We speculate that phosphorylation of S400 might destabilize the NBD-β-SBD interface, as it engages in the network that contributes to docked conformation. Unlike DnaK, the allosteric landscape of HspA1 is restricted to the two-state model, as the addition of peptide doesn't stimulate ATPase activity like in DnaK, and to a lesser extent in Hsc70, the eukaryotic cytoplasmic variant[2]. Phosphorylation induced destabilization may change the allosteric landscape of HspA1.

There is consistent evidence, *in vivo* and *in vitro,* of this destabilization throughout this study. Phosphomimetic mutants of HspA1 showed a great amount of proteolysis during

purification which was curtailed with a heavy supplementation of protease inhibitors. Despite this, the yield of all mutant proteins was lower than WT. Some of the degradation was mitigated with the addition of ATP/ADP and a step imidazole wash. The vulnerability of the NBD is reduced as it is stabilized with nucleotide, as the presence of either ATP or ADP because both favor the domain-docked conformation of HspA1. Degradation observed in the elution fractions was often present alongside a strong band for SBD, and both can be explained by the fact that the C-terminal end of the SBD is accessible to being proteolytically cleaved. In addition, there is potential for interactions between the cleaved SBD and the exposed linker regions of phosphomimetic constructs[39]. It is still surprising to see much of the stable mutant protein elute at 10% of the imidazole concentration used for elution.

Through limited proteolysis experiments we demonstrated that phosphorylation destabilizes HspA1 (Fig 2.3A). The appearance of the NBD and SBD bands as a function of time reports on cleavage at the linker. The SBD band is scarce in all constructs as lack of substrate leaves the SBD unstable. In the case of S385D/S400D, this linker cleavage gave rise to further proteolytic events throughout the protein. This indicates a global instability resulting from phosphomimetic substitutions at positions 385 and 400. The data we present, through fluorescence anisotropy-based binding experiments corroborates these findings. Mutants S400D and S385D/S400D showed lower substrate affinity than WT. Circular dichroism revealed that S385D/S400D, was structurally less similar to WT than the two single mutants, but both S400D and S385D/S400D are destabilized. This conclusion can be extracted despite the noisy data, which could be a result of the sample not being given enough time to reach thermal equilibration, or the data pitch is too high.

Surprisingly, the preliminary MD study performed suggests that phosphorylation at residue 400 alone shifts HspA1 towards the docked state. The short simulation suggests that upon phosphorylation of S400, interdomain contacts participating in the βSBD-NBD interface are strengthened. The RMSD suggests that P-Ser 400 restricts the dynamic range of the protein for residues encompassing a 15Å region around S400, but there are regions that do experience a change in fluctuation due to phosphorylation. It is possible that a 100ns trajectory might be too short to definitively ascertain the impact of phosphorylation on the conformational landscape of HspA1. For example, the RMSD trace of both WT and P- Ser 400 intersect twice, and then level off at the end of the simulation. Inspecting movement of individual residues reveals details that might otherwise be hidden in the RMSD profile. The perturbations S400D confers locally to the SBD and distally impact substrate binding. It is possible that the perturbance caused by this mutation enables the chaperone to reside in the docked state for longer, with fast exchange for substrate, resulting in high apparent K_D.

2.4 MATERIALS AND METHODS

2.4.1 Experimental Design

To investigate the allosteric effects of phosphorylation on the linker region of Human Hsp70, two serine residues at positions 385 and 400 were mutated to aspartate to mimic phosphorylation. A direct binding assay, limited digestion, circular dichroism, and thermal melts will be used to test the effects on biochemical function and allosteric behavior of the S385D/S400D mutant.

2.4.2 Design and Expression of HspA1 constructs

For all experiments, HspA1 constructs containing both the NBD and partially truncated SBD (1-555). This construct incorporates mutations L542Y and V553E to abolish intramolecular tail-binding resulting from α-helical bundle and disordered C-terminus deletion. In addition, the T204A mutation is included to decreases ATP hydrolysis rate while preserving the ATP-induced conformational changes. This construct is referred to as WT* in this text. The His_6-tag is fused to the N-terminus end, followed by a tobacco etch virus (TEV) protease cleavage site. The pMCSG7 plasmid encoding wild-type HspA1 is a gift from Dr. Jason Gestwicki (UCSF). Truncations and mutations were introduced using site-directed mutagenesis.

Human Hsp70 has been shown to have high affinity for clathrin-derived peptide, QL (QLLMTAG, which was identified to be an endogenous substrate of the Hsp70 family by Ungewickell[40]. The QL peptide is used as a substrate for HspA1 in this study to compare binding affinities between WT* and phosphomimetic mutant, S385D/S400D.

Unlabeled HspA1 WT* and S385D/S400D were transformed into and over-expressed in Rosetta (DE3) cells. Cells were grown in Luria-Bertani (LB) medium (10 g/L of Bacto tryptone, 5 g/L of yeast extract, and 5 g/L of NaCl) and 100 μg/mL ampicillin at 37˚C, 200 rpm until

OD_{600} ~ 0.5. Cells were then supplemented with 20mM Proline and 300mM NaCl. Isopropyl β-D-1-thiogalactopyranoside (IPTG) was added at 0.6M to induce overexpression 30 minutes afterwards followed by incubation at 28˚C for 16 hours.

Cells were then harvested and resuspended in His-binding buffer (50 mM Tris-HCl (pH 8.0), 500 mM NaCl, 10 mM Imidazole, pH 8.0). Prior to lysis, cells were supplemented with protease inhibitors aprotinin (2µg/mL), phenylmethylsulfonyl fluoride (PMSF), leupeptin (10µM), and pepstatin (1µM). Lysate was centrifuged at 20,000 rpm for 45 minutes at 4˚C to separate soluble from insoluble fraction. The soluble fraction was used for subsequent immobilized metal affinity chromatography (IMAC) purification.

2.4.3 Purification of HspA1 constructs

HspA1 constructs were purified using a 20 mL column containing nickel (II) nitrilotriacetic acid (Ni-NTA) Agarose (Thermo Fisher Scientific) in the ÄKTA Prime Plus FPLC System (GE, Amersham) at 4˚C. Supernatant was treated 0.1 mM AEBSF and PMSF, 2µg/mL aprotinin, 10µM leupeptin, and 1µM pepstatin before being loaded onto the Ni-NTA affinity column. Non-specifically bound proteins were extensively washed from the column using His-binding buffer. A second wash with 2mM ATP was passed through the column to remove contaminating substrates from the protein. His-Eluting buffer (50 mM Tris-HCl (pH 8.0), 500 mM NaCl, 300 mM imidazole) was used to elute the bound protein. The His_6-tag on all HspA1 constructs was cleaved with His_6-tagged TEV protease at 4˚C overnight. Optimal cleavage with TEV protease requires a sample with < 2 M urea, < 50 mM imidazole, and absence of any cysteine protease inhibitors. Elution fractions from previous Nickel IMAC were buffer exchanged to 50mM Tris, 500mM NaCl using a 15 mL 30 MWCO Amicon Ultra Centrifugal Filter. After cleavage, a second iteration of Ni-NTA affinity chromatography was

used to remove His_6-HspA1 and His_6-TEV protease from the cleaved HspA1. 2mM ATP was added to the sample before being loaded onto the Ni-NTA resin. Column was extensively washed with Buffer A (50mM Tris, 500mM NaCl) and His_6-HspA1 and His_6-TEV protease were eluted with 5 CV of His-Eluting Buffer. The flow through protein is buffer exchanged into HMK buffer (20 mM HEPES, 10 mM $MgCl_2$, 100 mM KCl pH 7.6). Phosphomimetic S385D/S400D was additionally passed through a Superdex 75 16/60 (GE Healthcare) gel filtration column in HMK to remove any remaining impurities. All purified constructs were concentrated and stored at -80˚C. Presence of protein was detected after each purification step via a 12% acrylamide SDS-PAGE and visualized with Coomassie stain.

2.4.4 Limited Proteolysis

Limited proteolysis was performed on all HspA1 constructs: WT*, S385D, S400D, and S385D/S400D. HspA1 (20μM) was pre-incubated overnight at 4˚C in HMK buffer supplemented with 5mM $CaCl_2$, 5mM DTT, and 5mM ADP. Proteolysis was initiated by adding proteinase K to a final concentration of 0.01 mg/mL at 20˚C. 10uL aliquots were taken at 5-minute intervals (5 mins, 10 mins, 15 mins) and quenched with 100μM PMSF. Samples with and without the addition of proteinase K were visualized by SDS-PAGE and Coomassie stain. The bands on the SDS-PAGE were analyzed via densitometry to quantify bands corresponding to the original construct and proteolyzed products: NBD and SBD.

2.4.5 Substrate binding assay

Substrate binding affinity of fluorescein isothiocyanate (FITC)-labeled peptide QL to HspA1 constructs was measured with fluorescence anisotropy as previously described[41]. FITC-QL peptide were purchased from Biomatik USA (Wilmington, DE). The assay was performed in

HMK buffer with 1mM DTT and 5mM ADP. FITC-QL was at a fixed concentration of 50nM and HspA1 was serially diluted between 0-35μM. 5 mM nucleotides were added for ADP and ATP-bound samples. ADP bound samples were incubated at 4˚C for 24 hours before reading. Fluorescent anisotropy was measured on a 384-well plate (Corning, NY) using the Biotek Synergy2 plate reader (Biotek, USA) with excitation at 485 nm and emission at 528 nm at 25˚C. Measurements were performed as a technical triplicate. Anisotropy is calculated as previously described, using the equation:

$$\text{Anisotropy}(r) = \frac{(I_{VV} - G * I_{VH})}{(I_{VV} + 2 * G * I_{VH})}$$

$$G = \frac{I_{HV}}{I_{HH}}$$

where I_{VV} and I_{VH} are the orientations of the polarizers as denoted on the plate reader software (Table 1), and G is the instrument specific sensitivity ratio towards vertically and horizontally polarized light.

The fraction of FITC-QL bound to HspA1 was calculated by the equation:

$$Fraction\ bound\ (f_B) = \frac{(r_{obs} - r_F)}{(r_B - r_F)}$$

where r_{obs} is the observed anisotropy of FITC-peptide at certain concentration of HspA1; r_F is the anisotropy of the free FITC-peptide, which is obtained at zero concentration of HspA1; r_B is the anisotropy of FITC-peptide bound to HspA1, which is determined from the anisotropy in the plateau of the binding curve at high concentration HspA1. The data were fitted to the following quadratic:

$$f_B = \frac{([P_T] + K_D + [S_T]) - \sqrt{\{([P_T] + [S_T] + K_D)^2 - 4[P_T] * [S_T]\}}}{2 * [S_T]}$$

where f_B is fraction bound, P_T is the total protein concentration; S_T is the fixed FITC-QL concentration; K_D is the dissociation constant. All data was analyzed using Origin Pro.

2.4.6 Circular Dichroism

Measurements of all HspA1 constructs were taken as previously described using a Jasco J- 715 spectropolarimeter[41]. CD [mdeg] was recorded for wavelengths from 200-250nm for 3 accumulations each. Parameters include 0.2nm data pitch, 2.0 nm bandwidth, 2 sec response rate, and 50 nm/min scanning speed in a cell length of 0.1 cm. Thermal scans were taken between 25-95˚C at a 1˚C data pitch, 2.0 nm bandwidth, 4 sec response rate, 2˚C/min temperature slope. The wavelength monitored was 220nm. Measurements were taken at 25˚C in 10mM potassium phosphate pH 7.4, 100µM ADP with 1-2µM of protein. Values are reported in molar ellipticity.

2.4.7 Homology Modeling, Molecular visualization

A sequence alignment was executed between HspA1 and DnaK using Clustal Omega. ATP- bound state of HspA1 was built using ATP-bound DnaK (PDB 4b9q) as a template on the SWISS-MODEL web server.

2.4.8 Molecular Dynamics

An initial homology model of the ATP-bound state of HspA1 was built using full-length DnaK with bound J-domain (PDB: 5nro) as a template on the SWISS-MODEL web server. Dnak was relaxed without the presence of the J domain. Simulations were run on charmm36m forcefield, and TIP3P as a water molecule. Potassium and chloride ions were included at a concentration of 0.01M to solvate the water in a 13Å buffer region. Simulations were run on a

100ns timescale following this set up: Nose-Hoover thermostat (303.15 K), Parinello-Rahman barostat (1 bar), periodic boundary conditions, Particle Mesh Ewald summation for long-range electrostatics, timestep of 2 fs allowed by using LINCS to constrain vibrations of hydrogen-containing bonds. Trajectory frames were saved at an interval of 100ps; 1000 frames were used to calculate RMSD and RMSF.

CHAPTER 3

QUO VADIS?

3.1 Summary

We know the cell to heavily rely on molecular chaperone under stress. The expression of Hsp70 is substantially increased as a part of the cellular stress response. Conventionally, the regulation of Hsp70 is thought to occur through substrate binding, varying co-chaperone interaction, and tuning its allostery in addition to expression. With recently increased attention on the role PTMs play in the regulation of chaperones, there is an added layer of complexity to the chaperone system. While fundamental differences like residue changes are permanently modulate Hsp70 function, PTMs provide a temporary alternative. In addition to regulating allostery and Hsp70 binding partners and substrates, PTMs may also exercise control over Hsp70 oligomerization and localization[5].

We are particularly intrigued by the sites of phosphorylation that tickle allostery. The aim of this work was to expand a prior study that examined the functional and physiological effects of phosphorylating two residues that comprise key allosteric players of Hsp70s: the linker and the substrate-binding domain. Sites S385 and S400D were identified to be in non-trivial locations upon closer inspection of Hsp70 structure. Previous work done in the lab further validated that S400D participates in a network of allosterically indispensable residues. This established a structural basis for the involvement of these residues in interdomain allostery.

Changes in the allosteric landscape of HspA1 were detected firstly by monitoring ADP-dependent substrate binding affinity and proteolysis experiments. Moreover, both S400D and S385D/S400D were destabilized upon heating. Ergo, we propose that phosphorylation of S400 has chiefly contributes to the allosteric behaviors of S385D/S400D HspA1. A molecular

dynamics simulation offered insight into the plausible implications of PTMs on HspA1. Taken together with the other methods, we postulate that phosphorylation S400 shifts the chaperone to the docked state. Simultaneously, overall protein stability is compromised as a result of phosphorylation.

This work exposes the subtleties of the effects of PTMs on chaperones. We show that phosphorylation influences both allostery and stability of HspA1, proving necessary to look past a simplistic two-state model to assess the complexities of PTMs.

3.2 Future Directions

The two sites of phosphorylation preliminarily investigated in this study certainly reveal intriguing and unexpected ways in which Hsp70s can be regulated. While this work and other preceding it have provided a foundation for exploring the mechanistic ways in which phosphorylation, and PTMs in general, alter chaperone function.

For the sites detailed in this work, we took a biochemical route to analyze the impact on *in vitro* activity. While the data presented here tantalizes novel insight on the impact of S385 and S400D phosphorylation, testing the reproducibility of this data would prove beneficial. Moving forward, performing biochemical assays on mutant S385D will provide a more complete analysis of each single mutant's contributions to the perturbance of the chaperone's conformational balance. Circular Dichroism was performed once with three accumulations, but the thermal scans were not replicated due to a shortage of resources. Therefore, it is crucial that these experiments are repeated and tuned to this system to reduce noise. Possible solutions may be to slow scanning rate to allow the protein to reach thermal equilibrium, or to collect at fewer temps along the temperature slope. Additionally, for majority of the samples used in this work, a Bradford assay was used to measure protein concentration with Hsp70 as a standard previously calculated by

Wenli Meng, a Senior Research Fellow in our lab. Moving forward, precise concentration determination by amino acid analysis will be necessary to prevent any methods of biochemical and biophysical characterization from being undermined.

The current techniques used can be supplemented with thermal stability assays in conjunction with SYPRO, a fluorophore commonly used in pharmaceutics. This method would provide an efficient way to confirm the thermal stability of each mutant, and support results from circular dichroism. We took advantage of a computational model to reveal the origins of phosphorylation induced perturbations via MD simulations. In this case study, simulating the effects of modifications will bring valuable insight to the conformational space around the sites, and provide an effective visual for what local or global changes the chaperone might be tolerating. Performing this simulation on both phosphorylation sites in both ATP and ADP bound states of HspA1 will lend clarity to overall impact on the allosteric landscape. Additionally, computational modeling and simulation could serve as a foundation for an easily accessible tool used to probe future PTM sites.

The impact of phosphorylation on the allosteric network can be systematically probed through the analysis of chemical shift perturbations from methyl-TROSY NMR spectra. Our lab has successfully assigned Ile-δ methyl chemical shifts for the eukaryotic Hsp70s in both the ADP and ATP-bound states. By taking advantage of a specific methyl labeling scheme, we can correlate observations like peak-walking, peak-broadening, and peak-splitting with the chaperone's allosteric behaviors to pinpoint sectors that are being perturbed by phosphorylation.

Most importantly, it would be negligent to disregard the phosphorylation mediated function of Hsp70 in a cellular context. Lim et al. report augmentation of cell proliferation in cells that ectopically express the mutant S385D/S400D and increased colony growth in a cell

viability assay, arguing that the cancer cells benefit from the phosphorylation of Hsp70 as it allows them to propagate rapidly. Their observations of high mutant refolding rates and increased substrate affinities follows this reasoning. From our data it's difficult to affirmatively attribute high substrate affinity with the S385D/S400D phosphomimetic, therefore we speculate there might be additional extrinsic factors promoting cell growth when the phosphomimetic mutant is ectopically expressed.

It can be argued that a higher K_D for the phosphomimetic suggests that Hsp70s role as holdase is more transient when phosphorylated. As the K_D increases, the k_{off} rate also increases, allowing the chaperone to bind to a multitude of clients. Meanwhile, the clients are still being shuttled to subsequent chaperones in the network, accumulating an overall increase in productivity of stably folded substrates. This theory offers a possible reconciliation between the disparate substate affinity observations and *in vivo* augmentation of cell viability between this work and the Lim et al. publication.

In addition, the assumption that sites 385 and 400 undergo concomitant phosphorylation underlies the basis of this work, but it is unclear if the two sites are differentially phosphorylated. There is no clear evidence that that S385D/S400D represents a pathological state of HspA1. Furthermore, whether both sites are accessible to the phosphorylating kinase is still under debate. If one site is more susceptible to phosphorylation, a see-saw effect on allostery will be observed. An imbalance in the energetic landscape that modulates allostery might allow temporary interconversion of HspA1 to another cytoplasmic Hsp70 isoform. Ultimately, the effects of phosphorylation on the linker regions of Hsp70 will be clarified upon a more robust integration of functional and *in vivo* studies.

The function of Hsp70 in protein quality control is not isolated. The HSP superfamily works in a concerted fashion to assist a client in reaching its native state. In addition to folding polypeptides fold, Hsp70 is also often an intermediary chaperone in a larger cascade (ref). Lim et al posit that post-translational modifications may preclude other co-chaperones such as Hsp40, Hsp90, and Hsp110 to name a few, from partnering with the 70. Ergo, an unsuccessful transition of substrate between chaperones presents a possible increase in the number of unsuccessful folding reactions. It would be interesting to identify the cellular interactions that the phosphorylated variants of HspA1 are involved. Building an elaborate interactome will supplement the work we have already done and shed light on the global consequences of phosphorylation.

APPENDIX

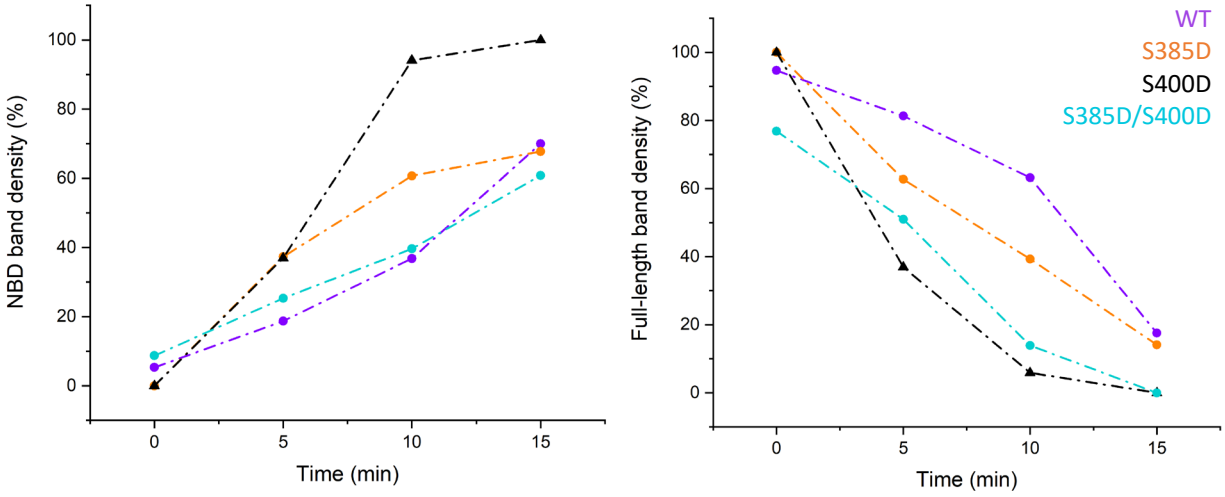

Figure A1. Nucleotide-binding domain and full-length band intensities over 15 min proteolysis experiment. NBD band intensity increases as a function of time as the full-length band decreases.

Table 2. Polarizer orientation used for fluorescence anisotropy measurements.

Measurement name	Excitation Polarizer	Emission Polarizer
I_{VV}	0˚	0˚
I_{VH}	0˚	90˚
I_{HV}	90˚	0˚
I_{HH}	90˚	90˚

*Measurement name corresponds to the intensity (I) with the excitation polarizer at X˚ and emission polarizer at Y˚

BIBLIOGRAPHY

1. Dill, K. A. & Chan, H. S. From Levinthal to pathways to funnels. *Nat. Struct. Biol.* **4**, 10–19 (1997).
2. Ellis, R. J. & Hartl, F. U. Principles of protein folding in the cellular environment. *Curr. Opin. Struct. Biol.* **9**, 102–110 (1999).
3. Dobson, C. M. Protein folding and misfolding. *Nature* **426**, 884–890 (2003).
4. Hardesty, B. & Kramer, G. Folding of a nascent peptide on the ribosome. *Prog. Nucleic Acid Res. Mol. Biol.* **66**, 41–66 (2001).
5. Rosenzweig, R., Nillegoda, N. B., Mayer, M. P. & Bukau, B. The Hsp70 chaperone network. *Nat. Rev. Mol. Cell Biol.* **20**, 665–680 (2019).
6. Hartl, F. U. & Hayer-Hartl, M. Molecular chaperones in the cytosol: from nascent chain to folded protein. *Science* **295**, 1852–1858 (2002).
7. Mayer, M. P. Hsp70 chaperone dynamics and molecular mechanism. *Trends Biochem. Sci.* **38**, 507–514 (2013).
8. Zuiderweg, E. R. P. *et al.* Allostery in the Hsp70 chaperone proteins. *Top. Curr. Chem.* **328**, 99–153 (2013).
9. Bukau, B., Weissman, J. & Horwich, A. Molecular Chaperones and Protein Quality Control. *Cell* **125**, 443–451 (2006).
10. Rüdiger, S., Buchberger, A. & Bukau, B. Interaction of Hsp70 chaperones with substrates. *Nat. Struct. Mol. Biol.* **4**, 342–349 (1997).
11. Rudiger, S. Substrate specificity of the DnaK chaperone determined by screening cellulose-bound peptide libraries. *EMBO J.* **16**, 1501–1507 (1997).

12. Van Durme, J. *et al.* Accurate prediction of DnaK-peptide binding via homology modelling and experimental data. *PLoS Comput. Biol.* **5**, e1000475 (2009).

13. Zhu, X. *et al.* Structural Analysis of Substrate Binding by the Molecular Chaperone DnaK. *Science* **272**, 1606–1614 (1996).

14. Marcinowski, M. *et al.* Conformational Selection in Substrate Recognition by Hsp70 Chaperones. *J. Mol. Biol.* **425**, 466–474 (2013).

15. Bhattacharya, A. *et al.* Allostery in Hsp70 Chaperones Is Transduced by Subdomain Rotations. *J. Mol. Biol.* **388**, 475–490 (2009).

16. Zhang, Y. & Zuiderweg, E. R. P. The 70-kDa heat shock protein chaperone nucleotide-binding domain in solution unveiled as a molecular machine that can reorient its functional subdomains. *Proc. Natl. Acad. Sci. U. S. A.* **101**, 10272–10277 (2004).

17. Kityk, R., Kopp, J., Sinning, I. & Mayer, M. P. Structure and Dynamics of the ATP-Bound Open Conformation of Hsp70 Chaperones. *Mol. Cell* **48**, 863–874 (2012).

18. Swain, J. F. *et al.* Hsp70 Chaperone Ligands Control Domain Association via an Allosteric Mechanism Mediated by the Interdomain Linker. *Mol. Cell* **26**, 27–39 (2007).

19. Wilbanks, S. M., Chen, L., Tsuruta, H., Hodgson, K. O. & McKay, D. B. Solution small-angle x-ray scattering study of the molecular chaperone Hsc70 and its subfragments. *Biochemistry* **34**, 12095–12106 (1995).

20. Clerico, E. M. *et al.* Hsp70 molecular chaperones: multifunctional allosteric holding and unfolding machines. *Biochem. J.* **476**, 1653–1677 (2019).

21. Lai, A. L. *et al.* Key features of an Hsp70 chaperone allosteric landscape revealed by ion-mobility native mass spectrometry and double electron-electron resonance. *J. Biol. Chem.* **292**, 8773–8785 (2017).

22. Bertelsen, E. B., Chang, L., Gestwicki, J. E. & Zuiderweg, E. R. P. Solution conformation of wild-type E. coli Hsp70 (DnaK) chaperone complexed with ADP and substrate. *Proc. Natl. Acad. Sci. U. S. A.* **106**, 8471–8476 (2009).

23. Zhuravleva, A., Clerico, E. M. & Gierasch, L. M. An interdomain energetic tug-of-war creates the allosterically active state in Hsp70 molecular chaperones. *Cell* **151**, 1296–1307 (2012).

24. Qi, R. *et al.* Allosteric opening of the polypeptide-binding site when an Hsp70 binds ATP. *Nat. Struct. Mol. Biol.* **20**, 900–907 (2013).

25. English, C. A., Sherman, W., Meng, W. & Gierasch, L. M. The Hsp70 interdomain linker is a dynamic switch that enables allosteric communication between two structured domains. *J. Biol. Chem.* **292**, 14765–14774 (2017).

26. Yang, J., Nune, M., Zong, Y., Zhou, L. & Liu, Q. Close and Allosteric Opening of the Polypeptide-Binding Site in a Human Hsp70 Chaperone BiP. *Structure* **23**, 2191–2203 (2015).

27. Zhuravleva, A. & Gierasch, L. M. Substrate-binding domain conformational dynamics mediate Hsp70 allostery. *Proc. Natl. Acad. Sci. U. S. A.* **112**, E2865-2873 (2015).

28. Vogel, M., Bukau, B. & Mayer, M. P. Allosteric regulation of Hsp70 chaperones by a proline switch. *Mol. Cell* **21**, 359–367 (2006).

29. Meng, W., Clerico, E. M., Mcarthur, N. & Gierasch, L. M. Allosteric landscapes of eukaryotic cytoplasmic Hsp70s are shaped by evolutionary tuning of key interfaces. doi:10.1073/pnas.1811105115.

30. Kityk, R., Kopp, J. & Mayer, M. P. Molecular Mechanism of J-Domain-Triggered ATP Hydrolysis by Hsp70 Chaperones. *Mol. Cell* **69**, 227-237.e4 (2018).

31. Kampinga, H. H. *et al.* Function, evolution, and structure of J-domain proteins. *Cell Stress Chaperones* **24**, 7–15 (2019).

32. Liberek, K., Marszalek, J., Ang, D., Georgopoulos, C. & Zylicz, M. Escherichia coli DnaJ and GrpE heat shock proteins jointly stimulate ATPase activity of DnaK. *Proc. Natl. Acad. Sci.* **88**, 2874–2878 (1991).

33. Behl, C. Breaking BAG: The Co-Chaperone BAG3 in Health and Disease. *Trends Pharmacol. Sci.* **37**, 672–688 (2016).

34. Porter, C. M., Truman, A. W. & Truttmann, M. C. Post-translational modifications of Hsp70 family proteins: Expanding the chaperone code. (2020) doi:10.1074/jbc.REV120.011666.

35. Lim, S., Kim, D. G. & Kim, S. ERK-dependent phosphorylation of the linker and substrate-binding domain of HSP70 increases folding activity and cell proliferation. *Exp. Mol. Med.* **51**, (2019).

36. Ryan, B. J. & Henehan, G. T. Avoiding Proteolysis During Protein Purification. in *Protein Chromatography: Methods and Protocols* (eds. Walls, D. & Loughran, S. T.) 53–69 (Springer, 2017). doi:10.1007/978-1-4939-6412-3_4.

37. Sreerama, N. & Woody, R. W. Computation and Analysis of Protein Circular Dichroism Spectra. in *Methods in Enzymology* vol. 383 318–351 (Academic Press, 2004).

38. Heinig, M. & Frishman, D. STRIDE: a web server for secondary structure assignment from known atomic coordinates of proteins. *Nucleic Acids Res.* **32**, W500–W502 (2004).

39. Aprile, F. A. *et al.* Hsp70 Oligomerization Is Mediated by an Interaction between the Interdomain Linker and the Substrate-Binding Domain. *PLoS ONE* **8**, e67961 (2013).

40. Ungewickell, E. The 70-kd mammalian heat shock proteins are structurally and functionally related to the uncoating protein that releases clathrin triskelia from coated vesicles. *EMBO J.* **4**, 3385–3391 (1985).

41. Montgomery, D. L., Morimoto, R. I. & Gierasch, L. M. Mutations in the substrate binding domain of the Escherichia coli 70 kDa molecular chaperone, DnaK, which alter substrate affinity or interdomain coupling. *J. Mol. Biol.* **286**, 915–932 (1999).